

Floquet dynamical decoupling at zero bias

Peng Xu^{1,2,*} and Jun Zhang³

¹*School of Physics, Zhengzhou University, Zhengzhou 450001, China*

²*Institute of Quantum Materials and Physics, Henan Academy of Sciences, Zhengzhou 450046, China*

³*School of Physics and Technology, Wuhan University, Wuhan, Hubei 430072, China*



(Received 4 July 2023; accepted 13 November 2023; published 27 November 2023)

Dynamical decoupling (DD) is an efficient method to decouple systems from environmental noise and to prolong the coherence time of systems. In contrast to discrete and continuous DD protocols in the presence of bias field, we propose a Floquet DD at zero bias to perfectly suppress both the zeroth and first orders of noises according to the Floquet theory. Specifically, we demonstrate the effectiveness of this Floquet DD protocol in two typical systems including a spinor atomic Bose-Einstein condensate decohered by classical stray magnetic fields and a semiconductor quantum dot electron spin coupled to nuclear spins. Furthermore, our protocol can be used to sense high-frequency noises. The Floquet DD protocol we propose shines light on low-cost and highly portable DD technics without bias field and with low controlling power, which may have wide applications in quantum computing, quantum sensing, nuclear magnetic resonance, and magnetic resonance imaging.

DOI: [10.1103/PhysRevB.108.174310](https://doi.org/10.1103/PhysRevB.108.174310)

I. INTRODUCTION

Systems that are not sufficiently isolated inevitably couple to environments, resulting in finite coherence time, finite lifetime, and particle loss [1–4]. The fidelity of entangled-state preparations and the reliability of quantum-gate operations will be decreased [5–9], leading to destructive effects on many quantum applications, such as quantum communication [10], quantum teleportation [11,12], and quantum computing [13,14]. Therefore, it is crucial to suppress these destructive channels in experiments. However, the time scale of decoherence induced by noises or interactions is much shorter than other destructive channels. Thus, suppressing the decoherence channel and prolonging the coherence time is the first challenge in experiments [15–20].

Dynamical decoupling (DD) is a useful mechanism to prolong the coherence time of systems and to decouple systems from both classical and quantum noises [21–23]. It was proposed by Hahn [24] as spin echo, then developed into various forms, such as Carr-Purcell-Meiboom-Gill [25,26], periodic DD [27], concatenated DD (CDD) [27,28], Uhrig DD, concatenated Uhrig DD (CUDD) [29,30], and uniaxial DD [31]. The DD protocols mentioned above are the discrete type with strong strength of control pulses. To decrease the controlling power, continuous DD protocols have been proposed [32–42]. Recently, these DD protocols have been widely applied to various systems, such as quantum dots (QDs) [43,44], nitrogen-vacancy centers [17,38,41], trapped ions [19,20,37], and superconducting quantum interference devices [16,45,46]. The coherence time of systems is significantly improved in experiments. However, both discrete and continuous DD protocols require a large bias field, which

makes the experimental setups high cost and low portability. Additionally, there are potential tasks to decouple systems from noises, to sense noises, and to coherently stabilize quantum gates without bias [47–52]. Thus, it is necessary and significant to propose a protocol aiming at suppressing the decoherence channel and sensing high-frequency noises at zero bias. Even though the continuous DD with reversed amplitudes yielding effectively zero bias was experimentally demonstrated [45], we here propose a method with the true zeroness of the applied bias.

In this paper, we propose a method named Floquet DD at zero bias to decouple systems from environments. We first analytically obtain the effective Hamiltonian under Floquet DD based on the Floquet theory, which demonstrates our protocol can not only suppress the zeroth order of noises but prevent systems from being decohered by the first order of noises. Second, numerical simulations confirm the commendable performance of our protocol in a spinor Bose-Einstein condensate (BEC) decohered by stray magnetic fields (classical noises) and in a semiconductor QD electron spin qubit decohered by nuclear spins (quantum noises). Our results can be applied to research in low control fields and zero bias in nuclear magnetic resonance and quantum sensing beyond the standard quantum limit.

II. FLOQUET DD

Before we discuss the Floquet DD, we briefly review existing DD protocols. To compare our method with these protocols, we depict them in the toggling frame of bias since there is no bias in our method intrinsically. The simplest discrete DD, i.e., spin echo, is shown in Fig. 1(a). The control Hamiltonian is $\hat{H}_c = \Omega \delta(t - nT) \hat{J}_x$, with controlling strength satisfying $\int_{nT-\epsilon/2}^{nT+\epsilon/2} \Omega \delta(t - nT) dt = \pi$; then noises along the

*2014202020003@whu.edu.cn

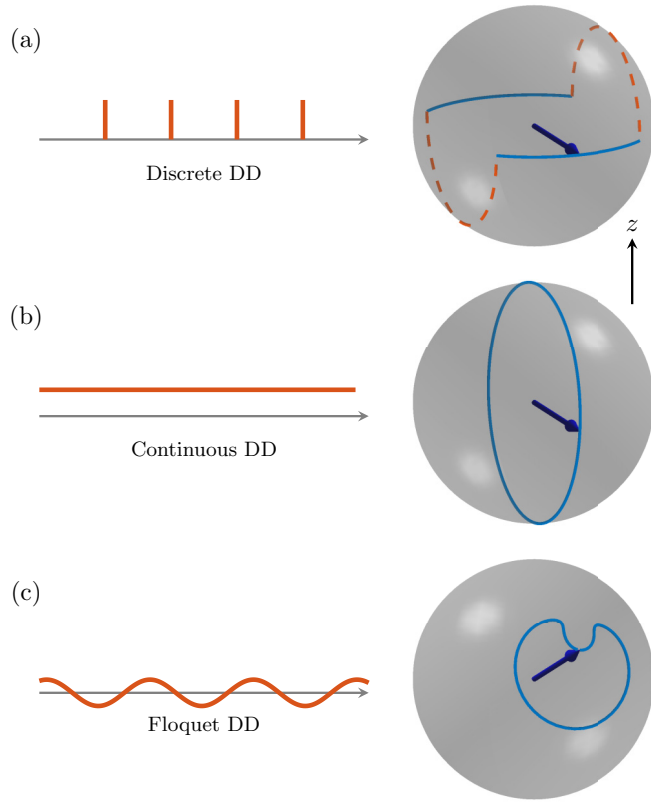


FIG. 1. Schematics for different dynamical decoupling (DD) protocols. The control is along the x axis, and noises are along the z axis, $b_z \in [-b_m, b_m]$. The typical DD protocols are shown in the left panels, while the corresponding evolutions are shown in the right panels. (a) Discrete DD. (b) Continuous DD. (c) Floquet DD.

z axis $\hat{H}_z = b_z \hat{J}_z$ with strength $b_z \in [-b_m, b_m]$ are suppressed. As a result, the spin returns to its initial state after one period, as shown in the right panel of Fig. 1(a). A typical continuous DD is shown in Fig. 1(b). The control Hamiltonian is $\hat{H}_c = \Omega \hat{J}_x$; then the system is decoupled from noises under the condition $\Omega \gg b_m$. The evolution trajectory is shown in the right panel of Fig. 1(b), which forms a closed circle.

The Floquet DD protocol we propose is shown in Fig. 1(c). The control Hamiltonian is $\hat{H} = \Omega \cos(\omega t + \varphi) \hat{J}_x$, with controlling strength Ω and frequency ω ; then the evolution of systems coupled to longitudinal magnetic noises is governed by

$$\hat{H} = b_z \hat{J}_z + \Omega \cos(\omega t + \varphi) \hat{J}_x, \quad (1)$$

where we assume $|b_z| \leq b_m$. After applying a rotating wave transformation $\hat{U} = \exp[i \int_0^t \Omega \cos(\omega \tau + \varphi) \hat{J}_x d\tau]$, the Hamiltonian becomes

$$\hat{H}_r = b_z \sum_{n=-\infty}^{\infty} \{ \mathcal{J}_{2n} \exp[i2n(\omega t + \varphi)] \hat{J}_z - i \mathcal{J}_{2n+1} \exp[i(2n+1)(\omega t + \varphi)] \hat{J}_y \}, \quad (2)$$

where \mathcal{J}_n is the n th-order Bessel function of Ω/ω . When ω is larger than b_m , we can use the high-frequency expansion to

obtain the Floquet effective Hamiltonian:

$$\hat{H}_{\text{eff}} = \hat{H}^{(0)} + \sum_{n \neq 0} \left(\frac{[\hat{H}^{(n)}, \hat{H}^{(-n)}]}{2n\omega} - \frac{[\hat{H}^{(n)}, \hat{H}^{(0)}]}{n\omega} \right) + \dots,$$

where $\hat{H}^{(n)} = \frac{1}{T} \int_0^T \hat{H}(t) e^{-in\omega t} dt$. In the high-frequency limit, the rotating wave approximation, we can keep the expansion to the leading order:

$$\hat{H}_{\text{eff}} = b_z \mathcal{J}_0 \hat{J}_z. \quad (3)$$

When the ratio Ω/ω satisfies $\mathcal{J}_0(\Omega/\omega) = 0$, the zeroth order of noises about b_z is completely suppressed. Furthermore, because of $[\hat{H}^{(n)}, \hat{H}^{(-n)}] = 0$, the first order of longitudinal noises is also inhibited perfectly.

According to the above analysis, we conclude that both the zeroth and first orders of longitudinal noises are suppressed completely. However, in experiments, there may exist noises with random directions, i.e., stray magnetic fields. Thus, it is vital for Floquet DD to prevent systems from being decohered by stray magnetic fields. Fortunately, our protocol can be directly extended to suppress these noises. The Hamiltonian with controls in this situation is

$$\hat{H} = \mathbf{b} \cdot \hat{\mathbf{J}} + \sum_{\alpha=x,y} \Omega_\alpha \cos(\omega_\alpha t + \varphi_\alpha) \hat{J}_\alpha, \quad (4)$$

where we assume $|\mathbf{b}| \leq b_m$ and $\omega_x = \omega_y = \omega$ [53]. In the following, we apply a rotating wave transformation $\hat{U}^I = \exp[i \int_0^t \Omega_x \cos(\omega \tau + \varphi_x) \hat{J}_x d\tau]$, resulting in the Hamiltonian:

$$\hat{H}_r^I = \sum_{n=-\infty}^{\infty} \hat{H}^{(n)} e^{in\omega t}, \quad (5)$$

where

$$\begin{aligned} \hat{H}^{(0)} &= b_x \hat{J}_x + b_y \mathcal{J}_0 \hat{J}_y + b_z \mathcal{J}_0 \hat{J}_z - \Omega_y \mathcal{J}_1 \sin(\varphi_x - \varphi_y) \hat{J}_z, \\ \hat{H}^{(2n \neq 0)} &= b_y \mathcal{J}_{2n} \exp(i2n\varphi_x) \hat{J}_y + b_z \mathcal{J}_{2n} \exp(i2n\varphi_x) \hat{J}_z \\ &\quad + i \frac{\Omega_y}{2} (\mathcal{J}_{2n-1} \exp[i(2n-1)\varphi_x + \varphi_y]) \\ &\quad + \mathcal{J}_{2n+1} \exp[i(2n+1)\varphi_x - \varphi_y] \hat{J}_z \\ \hat{H}^{(2n+1)} &= i b_y \mathcal{J}_{2n+1} \exp[i(2n+1)\varphi_x] \hat{J}_z \\ &\quad - i b_z \mathcal{J}_{2n+1} \exp[i(2n+1)\varphi_x] \hat{J}_y \\ &\quad + \frac{\Omega_y}{2} (\mathcal{J}_{2n} \exp[i2n\varphi_x + \varphi_y]) \\ &\quad + \mathcal{J}_{2n+2} \exp[i(2n+2)\varphi_x - \varphi_y] \hat{J}_y, \end{aligned}$$

with $\mathcal{J}_n \equiv \mathcal{J}_n(\Omega_x/\omega)$. In the high-frequency limit $\omega \gg b_m, \Omega_y$ and $\mathcal{J}_0(\Omega_x/\omega) = 0$, the effective Hamiltonian becomes

$$\hat{H}_{\text{eff}}^I = b_x \hat{J}_x + \gamma \hat{J}_z, \quad (6)$$

with $\gamma = -\Omega_y \mathcal{J}_1 \sin(\varphi_x - \varphi_y)$. Then we apply another rotating wave transformation $\hat{U}^{II} = \exp(i\gamma \hat{J}_z t)$, which transforms the above Hamiltonian to

$$\hat{H}_r^{II} = b_x [\cos(\gamma t) \hat{J}_x - \sin(\gamma t) \hat{J}_y]. \quad (7)$$

In the rotating wave approximation $\gamma \gg b_m$, the effective Hamiltonian is finally obtained:

$$\hat{H}_{\text{eff}}^{\text{II}} = 0. \quad (8)$$

Thus, the zeroth order of stray magnetic fields is completely suppressed. Furthermore, according to the Floquet expansion, when $\varphi_x = \pi/2$ or $3\pi/2$ and $\varphi_y = 0$ or π , $\hat{H}^{(n)}$ is equal to $\hat{H}^{(-n)}$ in Eq. (5), thereby inhibiting the first order of noises about b_y, b_z . The first order of noises about b_x can also be inhibited by alternatively tuning $\varphi_y = 0$ or $\varphi_y = \pi$ for two nearest-neighboring intervals and ensuring $|\gamma|T/2 = 2n\pi$ in each interval [54]. Until now, we have demonstrated the complete suppression of both the zeroth and first orders of stray magnetic noises. Additionally, higher orders of noises are also slightly suppressed by small coefficients because of the high-order Bessel function. More significantly, the above discussions about classical magnetic fields are also valid for quantum noises, only regarding \mathbf{b} as the $\hat{\mathbf{b}}$ operator. In the following two sections, we numerically calculate two concrete examples to illustrate that our protocol is capable of suppressing both classical and quantum noises.

III. SUPPRESSING CLASSICAL NOISES IN A SPINOR BEC

As for classical noises, we consider an atomic spinor BEC in external stray magnetic fields. The system with controls is described by the Hamiltonian $\hat{H} = \mathbf{b} \cdot \hat{\mathbf{J}} + \sum_{\alpha=x,y} \Omega_{\alpha} \cos(\omega_{\alpha}t + \varphi_{\alpha}) \hat{J}_{\alpha}$ under the single-mode approximation [55–58], which is the same as Eq. (4). Here, $\hat{\mathbf{J}}$ is the total spin of the spinor BEC and \mathbf{b} are stray magnetic fields that are randomly distributed in a sphere with radius b_m . The controls are chosen along the x and y axes. The energy and the time units are b_m and b_m^{-1} , respectively.

As we have demonstrated based on the Floquet theory, stray magnetic fields b_x, b_y , and b_z are all suppressed to the second order. Thus, without loss of generality, we just show numerical simulations of $\langle \hat{J}_y \rangle$ in Fig. 2. Due to $\mathcal{J}_0(\Omega_x/\omega) = 0$, we set $r_0 \equiv \Omega_x/\omega \approx 2.4048$. Additionally, to satisfy the high-frequency expansion ($\omega > \Omega_y \simeq \gamma > b_m$) and the commensuration between two rotating wave transformations, we set $r_1 \equiv \omega/\gamma \in \mathbb{Z}, r_2 \equiv \gamma/b_m \in \mathbb{R}$. According to numerical results shown in Fig. 2(a), we find expectation values of \hat{J}_y approach J as r_1 and r_2 increase. In Fig. 2(b), we show five typical dynamics of $\langle \hat{J}_y \rangle$ under different controlling parameters, where blue circles depict the free induced decay (FID) without Floquet DD, and other colored lines show decoherence with Floquet DD. These numerical results indicate that the coherence time is significantly prolonged under controls even when the controlling strengths are slightly larger than the strength of noises. For example, when $r_1 = r_2 = 4$, the coherence time is dozens of times longer than that of FID based on the rough estimation, and when $r_1 = r_2 \geq 8$, the coherence time is clearly seen prolonged by 2 orders of magnitude, which is consistent with the theoretical analysis indicating that stray magnetic fields are suppressed to the second order $O(1/r_{1,2}^2)$. In experiments, the strength of stray magnetic field b_m is usually < 1 mG, that is, corresponding to 0.7 kHz and is further suppressed to $10 \mu\text{G}$ in a magnetic shielding room [59]. If we roughly consider $b_m = 0.7$ kHz and $r_1 = r_2 = 8$,

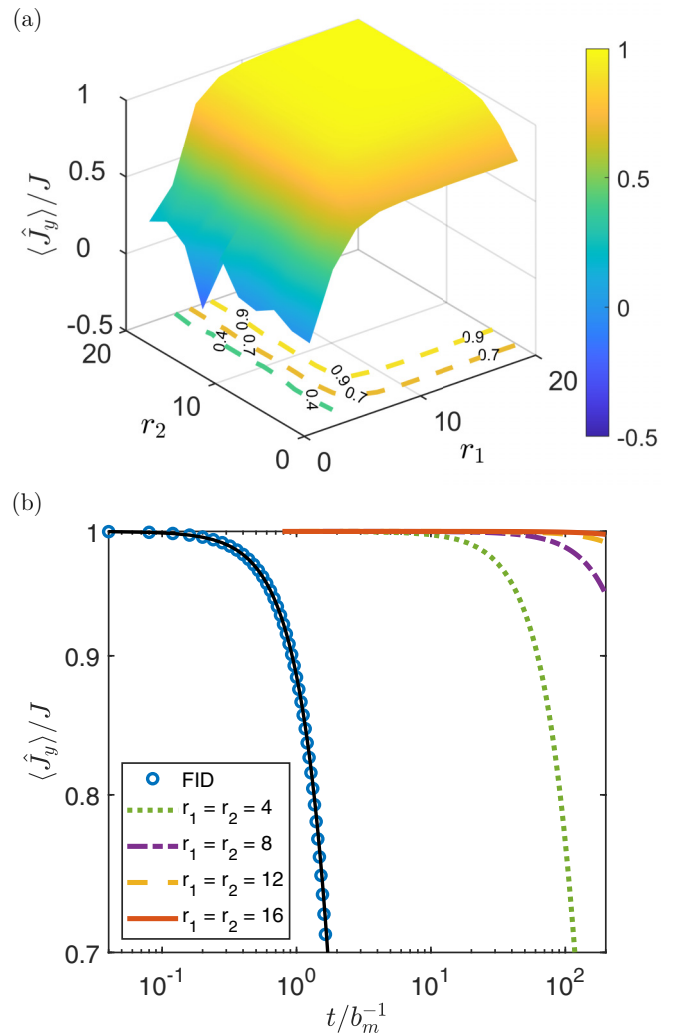


FIG. 2. Suppression of classical noises with Floquet dynamical decoupling (DD) in an atomic spinor Bose-Einstein condensate (BEC). (a) Expectation values of \hat{J}_y at time $t/b_m^{-1} = 200$ under different controlling parameters $r_1 = \omega/\gamma$ and $r_2 = \gamma/b_m$. (b) Dynamics of $\langle \hat{J}_y \rangle$ under several typical pairs of $\{r_1, r_2\}$, and free induced decay (FID) means there is no control. The black solid line mimics the decaying dynamics by $\exp(-\sigma^2 t^2)$, with $\sigma \approx 0.35b_m$. $\omega_x = \omega_y = \omega$, $\Omega_x = \omega r_0$, and $\Omega_y = \gamma/\mathcal{J}_1(r_0)$, with $\mathcal{J}_0(r_0) = 0$. Stray magnetic fields \mathbf{b} are randomly distributed in a sphere, and the radius of the sphere is b_m . The initial state is polarized along the y direction. J is the mean value of \hat{J}_y for the initial state.

the corresponding controlling parameters are $\omega \approx 44.8$ kHz, $\Omega_y \approx 10.8$ kHz, and $\Omega_x \approx 107.7$ kHz.

IV. SUPPRESSING QUANTUM NOISES IN A QD

As for quantum noises, which are intrinsically different from classical noises described by stochastic fields, they are treated by operators and their correlations. To illustrate the suppressing capability of our protocol, we consider a gate-defined GaAs semiconductor QD system, which is well described by a central electron spin decohered by surrounding nuclear spins [60–62]. The Hamiltonian of this system with N nuclear spins under two sequences of alternative controls

is $\hat{H} = \mathbf{S} \cdot \sum_{k=1}^N A_k \mathbf{I}_k + \sum_{\alpha=x,y} \Omega_\alpha \cos(\omega_\alpha t + \varphi_\alpha) \hat{S}_\alpha$, where \mathbf{S} and \mathbf{I} are the electron and nuclear spins, respectively, and both are assumed spin- $\frac{1}{2}$ for simplicity. In general, A_k is proportional to the local density of the electron at the position of the k th nucleus, $A_k = A_m \exp[-(x-x_0)^2/w_x^2 - (y-y_0)^2/w_y^2]$, a 2D ($N = 4 \times 3$) Gaussian form with effective widths $w_x/a_x = \frac{3}{2}$ and $w_y/a_y = 2$ (the lattice constant $a_{x,y}$), and a shifted center $x_0/a_x = 0.1$ and $y_0/a_y = 0.2$ [63]. The energy and time units are A_m and A_m^{-1} . Here, we neglect the interactions between nuclear spins because they are so small that the time scale of their dynamics is much longer than the decoherence time of the electron spin.

The meanings of controlling parameters r_0 , r_1 , and r_2 are the same as that in suppressing classical noises. We choose expectation values of \hat{S}_y as the witness for quantum noises suppression. The system evolution is simulated by the Chebyshev polynomial expansion [64]. According to Fig. 3(a), we find suppressing effects are increased as strengths of controlling parameters increase, which is like the behaviors in suppressing classical noises. However, based on Fig. 3(b), we find that the coherence time for suppressing quantum noises at $r_1 = r_2 = 8$ is like that for suppressing classical noises at $r_1 = r_2 = 4$. To compare these two different types of noises, we use the decaying dynamics $\exp(-\sigma^2 t^2)$ to mimic the processes of FID. We obtain $\sigma \approx 0.35 b_m$ for the classical noises and $\sigma \approx 0.35 \times 3A_m$ for the quantum noises. (The effective value of σ for quantum noises can be tuned by the initial distribution of nuclear spins [63].) Thus, in our numerical simulations, the controlling parameters for suppressing quantum noises should be larger than that for suppressing classical noises to achieve a similar coherence time. In experiments, A_m is typically equal to 10^{-4} μeV , that is, corresponding to 20 kHz [28,61,62]. Then the controlling parameters are $\omega \approx 1.28$ MHz, $\Omega_y \approx 0.31$ MHz, and $\Omega_x \approx 3.08$ MHz, if $r_1 = r_2 = 8$.

V. ROBUSTNESS OF FLOQUET DD

Although we have demonstrated the ability of Floquet DD in suppressing both classical and quantum noises, controlling fluctuations arising from power, frequency, and phase have not been considered. Based on current experimental conditions, we here mainly consider the fluctuation in controlling power Ω_α . Therefore, after applying the first rotating wave approximation, the Hamiltonian in Eq. (4) becomes $\hat{H}_{\text{eff}}^I = b_x \hat{J}_x + b'_y \hat{J}_y + b'_z \hat{J}_z + \gamma' \hat{J}_z$, with $b'_y = b_y \mathcal{J}_0(\Omega'_x/\omega)$, $b'_z = b_z \mathcal{J}_0(\Omega'_x/\omega)$, and $\gamma' = -\Omega'_y \mathcal{J}_1(\Omega'_y/\omega) \sin(\varphi_x - \varphi_y)$. The zeroth order of noises about b_y and b_z is suppressed to b'_y and b'_z , respectively. Then after applying the second rotating wave approximation, the above effective Hamiltonian becomes $\hat{H}_{\text{eff}}^{II} = b'_z \hat{J}_z - [\Omega'_y \mathcal{J}_1(\Omega'_y/\omega) - \Omega_y \mathcal{J}_1(\Omega_y/\omega)] \sin(\varphi_x - \varphi_y) \hat{J}_z$. Additionally, the second term $-[\Omega'_y \mathcal{J}_1(\Omega'_y/\omega) - \Omega_y \mathcal{J}_1(\Omega_y/\omega)] \sin(\varphi_x - \varphi_y) \hat{J}_z$ can be canceled by alternatively tuning $\varphi_y = 0$ or $\varphi_y = \pi$ for two nearest-neighboring intervals. Finally, the fluctuation of Ω_α leads to the residue of longitudinal magnetic noises b'_z , resulting in a shorter coherence time of spins in the $x-y$ plane than that along the z axis. Without loss of generality, we still choose $\langle \hat{F}_y \rangle$ as the witness of decoherence, where

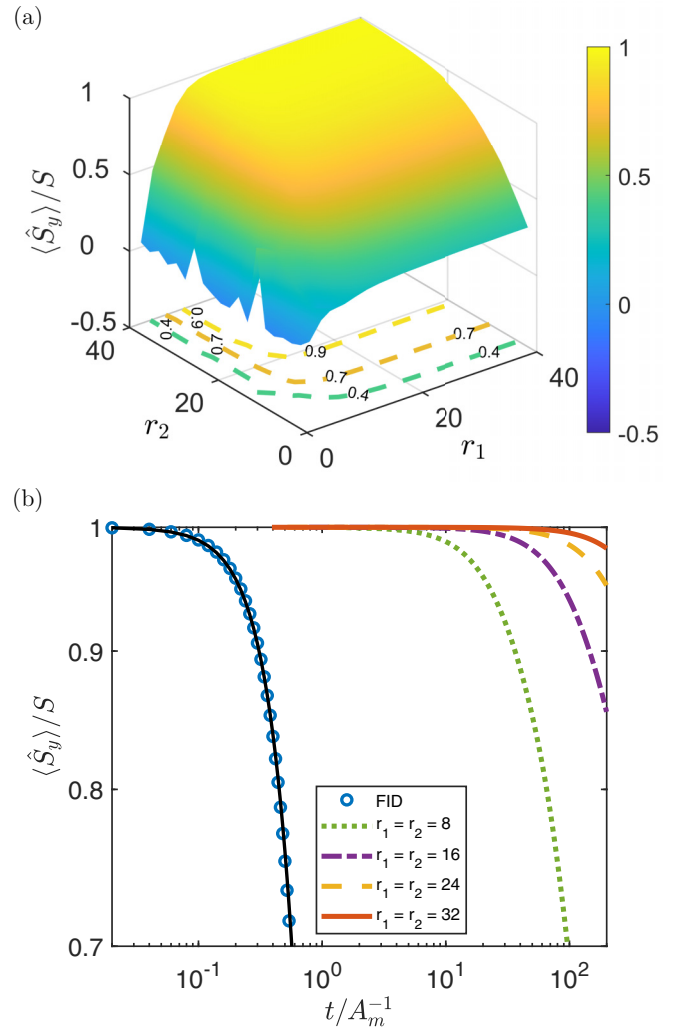


FIG. 3. Suppression of quantum noises with Floquet dynamical decoupling (DD) in a GaAs quantum dot (QD). (a) Expectation values of \hat{S}_y at time $t/A_m^{-1} = 200$ under different controlling parameters $r_1 = \omega/\gamma$ and $r_2 = \gamma/b_m$. (b) Dynamics of $\langle \hat{S}_y \rangle$ under several typical pairs of $\{r_1, r_2\}$, and free induced decay (FID) means there is no control. The black solid line mimics the decaying dynamics by $\exp(-\sigma^2 t^2)$, with $\sigma \approx 0.35 \times 3A_m$. $\omega_y = \omega_x = \omega$, $\Omega_x = \omega r_0$, and $\Omega_y = \gamma/\mathcal{J}_1(r_0)$, with $\mathcal{J}_0(r_0) = 0$. Coupling strengths of nuclear spin interactions are distributed in a two-dimensional (2D) (4×3) Gaussian form, $A_k = A_m \exp[-(x-x_0)^2/w_x^2 - (y-y_0)^2/w_y^2]$, with effective widths $w_x/a_x = \frac{3}{2}$ and $w_y/a_y = 2$ and a shifted center $x_0/a_x = 0.1$ and $y_0/a_y = 0.2$. The nuclear spins are initially randomly polarized on the Bloch sphere. The initial electronic spin is polarized along the y direction. S is the mean value of \hat{S}_y for the initial state.

\hat{F} denotes \hat{J} for classical noises and \hat{S} for quantum noises. Numerically, $r_0 \in [2.388, 2.417]$ approximately corresponds to 1.2% fluctuations of Ω_α , and the numerical simulations are shown in Fig. 4. Here, $\langle \hat{F}_y \rangle / F$ is still > 0.7 at time $t/b_m^{-1} = 200$ and $t/A_m^{-1} = 200$ for classical and quantum noises, respectively. Based on these results, we find these two kinds of noises are suppressed well, and the coherence time is still prolonged by 2 orders of magnitude even with fluctuation

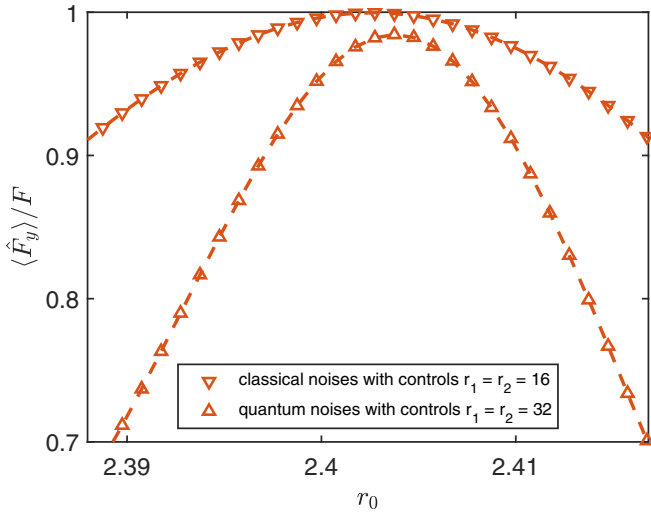


FIG. 4. Robustness of Floquet dynamical decoupling (DD) under fluctuation in controlling powers. $\langle \hat{F}_y \rangle$ means the expectation value of spins along the y axis at time $t/b_m^{-1} = 200$ ($t/A_m^{-1} = 200$). F denotes J (S) for classical (quantum) noises. $r_0 \in [2.388, 2.417]$ corresponds to 1.2% fluctuations of controlling power Ω_α . We set $r_1 = r_2 = 16$ and 32 for suppressing classical and quantum noises, respectively. The down (up) triangles depict the results for suppression of classical (quantum) noises with fluctuation of controlling power.

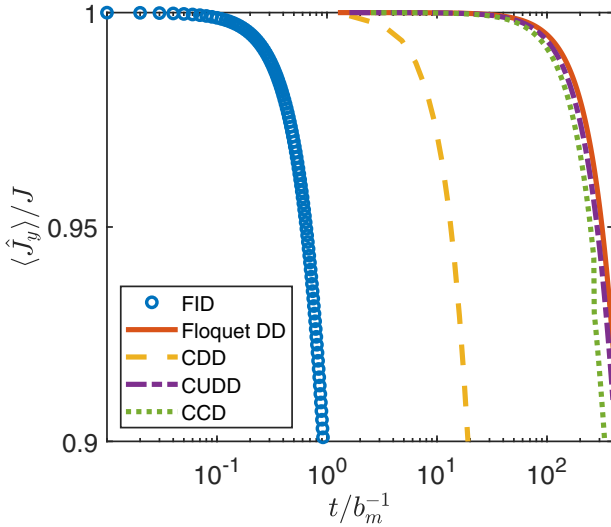


FIG. 5. Suppression of classical noises with Floquet dynamical decoupling (DD) and other existing DD protocols in an atomic spinor Bose-Einstein condensate (BEC). Dynamics of $\langle \hat{J}_y \rangle$ under parameters $r_1 = r_2 = 10$ in Floquet DD (solid line), and free induced decay (FID; circles) means there is no control. Both concatenated DD (CDD; dashed line) and concatenated Uhrig DD (CUDD; dot-dashed line) are concatenated once with fluctuation of bias $0.2 \text{ mG} = 0.2b_m$, pulse duration $20 \mu\text{s} \approx 0.02b_m^{-1}$ and pulse separation $\tau = 0.1b_m^{-1}$. Concatenated continuous DD (CCD; dotted line) under control Hamiltonian $\omega \hat{J}_z + 2\Omega_1 \cos(\omega t + \varphi_1) \hat{J}_x + 4\Omega_2 \cos(\omega t + \pi/2) \cos(\Omega_1 t + \varphi_2) \hat{J}_x$ satisfies the magic condition, and $\omega \gg \Omega_1$, $\Omega_1/\Omega_2 = 10$, and $\Omega_2/b_m = 10$, fluctuation of bias 0.2 mG . The initial state is polarized along the y direction. J is the mean value of \hat{J}_y for the initial state. Other parameters are the same as those shown in Fig. 2.

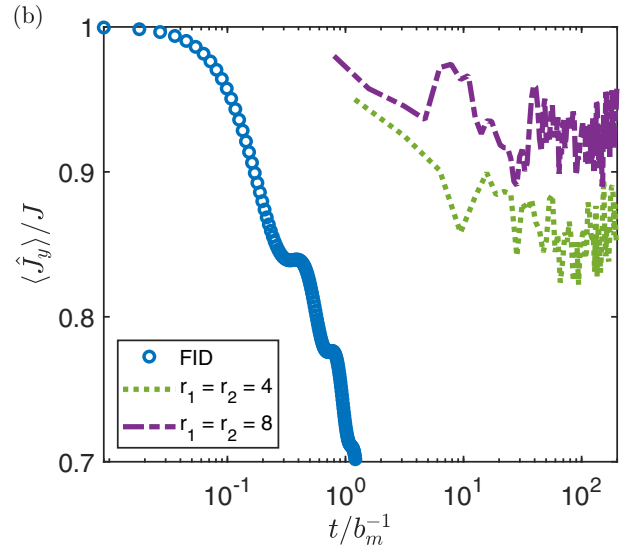
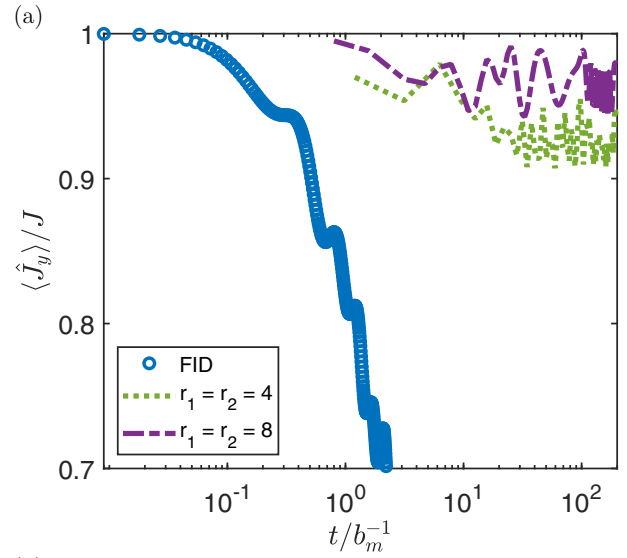


FIG. 6. Suppression of (a) pink noise and (b) Lorentzian noise with Floquet dynamical decoupling (DD) in an atomic spinor Bose-Einstein condensate (BEC). (a) and (b) Dynamics of $\langle \hat{J}_y \rangle$ under several typical pairs of $\{r_1, r_2\}$, and free induced decay (FID) means there is no control. The initial state is polarized along the y direction. J is the mean value of \hat{J}_y for the initial state. Other parameters are the same as those shown in Fig. 2.

in controlling powers, which manifests that our protocol is robust against controlling fluctuations.

VI. SUMMARY

We propose a Floquet DD protocol at zero bias to decouple systems from environmental noise. According to the theoretical analysis based on Floquet expansion, we find our protocol can not only suppress the zeroth order but the first order of noises. Additionally, we numerically calculate two systems including a spinor BEC in classical stray magnetic fields and a GaAs QD electron spin coupled to quantum nuclear spins. The numerical results of these two systems show our protocol significantly prolongs the coherence time and is robust against fluctuations in controlling powers. Furthermore, our protocol

can be used to sense noises with high frequency by detecting decoherence of systems. Our results suggest alternative low-cost and highly portable DD techniques without bias, which may find wide applications in quantum computing, quantum information processing, nuclear magnetic resonance, and magnetic resonance imaging.

ACKNOWLEDGMENTS

We thank Wenxian Zhang for invaluable discussions and Qi Yao for helpful discussions. This project is supported by the National Natural Science Foundation of China under Grants No. 12204428 and No. 12375023.

APPENDIX A: COMPARISONS BETWEEN OUR METHOD AND THE EXISTING DD PROTOCOLS

Although the notable merit of our method is the true zeroness of the applied bias, in this section, we compare our method to the existing DD protocols in terms of the effectiveness of noise suppression. Honestly speaking, the existing discrete DD protocols such as CDD [27] and CUDD [30] can suppress higher orders of noises if the DD is concatenated more times, while our method can only suppress both the zeroth and first orders of noises. However, if we focus on the lower orders (zeroth and first orders) of suppressing effect, i.e., both CDD and CUDD are concatenated once, our method has some advantages such as no fluctuation of bias and no error induced by the finite width of pulses. To compare the existing discrete DD protocols with our proposal numerically, the fluctuation of bias is set as 0.2 mG, and the pulse duration is set as 20 μs [65]. The numerical simulations are shown in Fig. 5, where parameters $r_1 = r_2 = 10$ in Floquet DD, and the pulse separation τ is set as $0.1b_m^{-1}$ in both CDD ($f_\tau x f_\tau y f_\tau x f_\tau z f_\tau x f_\tau y f_\tau x f_\tau x f_\tau y f_\tau x f_\tau z f_\tau x f_\tau y f_\tau x f_\tau$) and CUDD [$f_\tau y f_\tau f_\tau y f_\tau x (f_\tau y f_\tau f_\tau y f_\tau)^2 x f_\tau y f_\tau f_\tau y f_\tau$]. Other parameters are the same as that shown in Fig. 2. According to Fig. 5, we find that the CDD with fluctuation of bias and finite pulse width performs worse than the Floquet DD in

suppressing effect, while the performance of CUDD with these controlling errors is more robust than CDD, and the suppressing effect of CUDD is comparable with the Floquet DD. As for the continuous DD, there also exists the fluctuation of bias resulting in an extra controlling error. To compare the continuous DD with our proposal numerically, the fluctuation of bias is also set as 0.2 mG. The numerical result is depicted by the dotted line in Fig. 5, where we use the concatenated continuous DD (CCD) with control Hamiltonian $\omega \hat{J}_z + 2\Omega_1 \cos(\omega t + \varphi_1) \hat{J}_x + 4\Omega_2 \cos(\omega t + \pi/2) \cos(\Omega_1 t + \varphi_2) \hat{J}_x$ [36], which satisfies the magic condition to suppress both of the zeroth and first orders of noises demonstrated in our previous paper [39] and $\omega \gg \Omega_1$, $\Omega_1/\Omega_2 = 10$, $\Omega_2/b_m = 10$. According to the numerical result, we find the suppressing effect of CCD is slightly influenced by the fluctuation of bias.

APPENDIX B: SUPPRESSION OF COLORED NOISES WITH FLOQUET DD

To check the performance of Floquet DD under different types of colored noises, we calculate the spin dynamics for the BEC system under pink noise $S(\omega) \propto 1/\omega$ and Lorentzian noise $S(\omega) \propto \frac{\tau_{\text{corr}}}{1+(\omega-\omega_0)^2\tau_{\text{corr}}^2}$ with Floquet DD, where $S(\omega)$ is the power spectrum of the noise. The frequency of pink noise is numerically distributed in the range $[0.01, 1]\omega_c$, and the maximal strength of pink noise is $15b_m$, while the frequency of Lorentzian noise is in the $[-0.5 + \omega_0/\omega_c, 0.5 + \omega_0/\omega_c]\omega_c$ range, and the maximal strength of Lorentzian noise is also $15b_m$. In experiments, since the noise is mainly induced by the electromagnetic coils, the dominant frequency of the noise is 50 Hz. We here set $\omega_c = 500$ Hz, $\omega_0 = 50$ Hz, and $\tau_{\text{corr}} = 50$ ms. Other parameters are the same as those shown in Fig. 2. The numerical simulations are shown in Fig. 6. We find the suppressing effect of colored noises is more efficient than that of the static noise because the large-strength and low-frequency noise is significantly suppressed by our method, while the strength of high-frequency noise is very small.

-
- [1] M. A. Nielsen and I. Chuang, *Quantum Computation and Quantum Information* (Cambridge University Press, Cambridge, 2002).
 - [2] H.-P. Breuer and F. Petruccione, *The Theory of Open Quantum Systems* (Oxford University Press, Oxford, 2002).
 - [3] C. Gardiner and P. Zoller, *Quantum Noise: A Handbook of Markovian and Non-Markovian Quantum Stochastic Methods With Applications to Quantum Optics* (Springer-Verlag, Berlin, 2004).
 - [4] D. Suter and G. A. Álvarez, *Rev. Mod. Phys.* **88**, 041001 (2016).
 - [5] J. Ma, Y.-x. Huang, X. Wang, and C. P. Sun, *Phys. Rev. A* **84**, 022302 (2011).
 - [6] L. Aolita, F. de Melo, and L. Davidovich, *Rep. Prog. Phys.* **78**, 042001 (2015).
 - [7] P. Xu, S. Yi, and W. Zhang, *Phys. Rev. Lett.* **123**, 073001 (2019).
 - [8] E. Knill, *Nature (London)* **434**, 39 (2005).
 - [9] M. Abdelhafez, B. Baker, A. Gyenis, P. Mundada, A. A. Houck, D. Schuster, and J. Koch, *Phys. Rev. A* **101**, 022321 (2020).
 - [10] F. Bouchard, D. England, P. J. Bustard, K. L. Fenwick, E. Karimi, K. Heshami, and B. Sussman, *Phys. Rev. Appl.* **15**, 024027 (2021).
 - [11] S. Oh, S. Lee, and H.-w. Lee, *Phys. Rev. A* **66**, 022316 (2002).
 - [12] E. Jung, M.-R. Hwang, Y. H. Ju, M.-S. Kim, S.-K. Yoo, H. Kim, D. K. Park, J.-W. Son, S. Tamaryan, and S.-K. Cha, *Phys. Rev. A* **78**, 012312 (2008).
 - [13] P. Aliferis and J. Preskill, *Phys. Rev. A* **78**, 052331 (2008).
 - [14] M. Urbanek, B. Nachman, V. R. Pascuzzi, A. He, C. W. Bauer, and W. A. de Jong, *Phys. Rev. Lett.* **127**, 270502 (2021).
 - [15] H. Paik, S. K. Dutta, R. M. Lewis, T. A. Palomaki, B. K. Cooper, R. C. Ramos, H. Xu, A. J. Dragt, J. R. Anderson, C. J. Lobb *et al.*, *Phys. Rev. B* **77**, 214510 (2008).

- [16] B. Pokharel, N. Anand, B. Fortman, and D. A. Lidar, *Phys. Rev. Lett.* **121**, 220502 (2018).
- [17] M. H. Abobeih, J. Cramer, M. A. Bakker, N. Kalb, M. Markham, D. J. Twitchen, and T. H. Taminiua, *Nat. Commun.* **9**, 2552 (2018).
- [18] E. Bauch, S. Singh, J. Lee, C. A. Hart, J. M. Schloss, M. J. Turner, J. F. Barry, L. M. Pham, N. Bar-Gill, S. F. Yelin *et al.*, *Phys. Rev. B* **102**, 134210 (2020).
- [19] Y. Wang, M. Um, J. Zhang, S. An, M. Lyu, J.-N. Zhang, L.-M. Duan, D. Yum, and K. Kim, *Nature Photon* **11**, 646 (2017).
- [20] P. Wang, C.-Y. Luan, M. Qiao, M. Um, J. Zhang, Y. Wang, X. Yuan, M. Gu, J. Zhang, and K. Kim, *Nat. Commun.* **12**, 233 (2021).
- [21] U. Haeberlen, *High Resolution NMR in Solids Selective Averaging: Supplement 1 Advances in Magnetic Resonance* (Academic Press, New York, 1976).
- [22] M. Mehring, *Principles of High Resolution NMR in Solids* (Springer-Verlag, Berlin, 2012).
- [23] C. P. Slichter, *Principles of Magnetic Resonance* (Springer-Verlag, Berlin, 2013).
- [24] E. L. Hahn, *Phys. Rev.* **80**, 580 (1950).
- [25] H. Y. Carr and E. M. Purcell, *Phys. Rev.* **94**, 630 (1954).
- [26] S. Meiboom and D. Gill, *Rev. Sci. Instrum.* **29**, 688 (1958).
- [27] K. Khodjasteh and D. A. Lidar, *Phys. Rev. Lett.* **95**, 180501 (2005).
- [28] W. Zhang, N. P. Konstantinidis, V. V. Dobrovitski, B. N. Harmon, L. F. Santos, and L. Viola, *Phys. Rev. B* **77**, 125336 (2008).
- [29] G. S. Uhrig, *Phys. Rev. Lett.* **98**, 100504 (2007).
- [30] G. S. Uhrig, *Phys. Rev. Lett.* **102**, 120502 (2009).
- [31] Q. Yao, J. Zhang, X.-F. Yi, L. You, and W. Zhang, *Phys. Rev. Lett.* **122**, 010408 (2019).
- [32] F. F. Fanchini, J. E. M. Hornos, and R. d. J. Napolitano, *Phys. Rev. A* **75**, 022329 (2007).
- [33] F. F. Fanchini, J. E. M. Hornos, and R. d. J. Napolitano, *Phys. Rev. A* **76**, 032319 (2007).
- [34] A. Bermudez, P. O. Schmidt, M. B. Plenio, and A. Retzker, *Phys. Rev. A* **85**, 040302(R) (2012).
- [35] A. Z. Chaudhry and J. Gong, *Phys. Rev. A* **85**, 012315 (2012).
- [36] J. Cai, B. Naydenov, R. Pfeiffer, L. P. McGuinness, K. D. Jahnke, F. Jelezko, M. B. Plenio, and A. Retzker, *New J. Phys.* **14**, 113023 (2012).
- [37] N. Timoney, I. Baumgart, M. Johanning, A. Varón, M. B. Plenio, A. Retzker, and C. Wunderlich, *Nature (London)* **476**, 185 (2011).
- [38] X. Xu, Z. Wang, C. Duan, P. Huang, P. Wang, Y. Wang, N. Xu, X. Kong, F. Shi, X. Rong *et al.*, *Phys. Rev. Lett.* **109**, 070502 (2012).
- [39] J. Zhang, Y. Han, P. Xu, and W. Zhang, *Phys. Rev. A* **94**, 053608 (2016).
- [40] A. Stark, N. Aharon, T. Uden, D. Louzon, A. Huck, A. Retzker, U. L. Andersen, and F. Jelezko, *Nat. Commun.* **8**, 1105 (2017).
- [41] R. P. Anderson, M. J. Kewming, and L. D. Turner, *Phys. Rev. A* **97**, 013408 (2018).
- [42] M. Cai and K. Xia, *Phys. Rev. A* **106**, 042434 (2022).
- [43] J. Medford, L. Cywiński, C. Barthel, C. M. Marcus, M. P. Hanson, and A. C. Gossard, *Phys. Rev. Lett.* **108**, 086802 (2012).
- [44] B. Sun, T. Brecht, B. Fong, M. Akmal, J. Z. Blumoff, T. A. Cain, F. W. Carter, D. H. Finestone, M. N. Fireman, W. Ha *et al.*, *arXiv:2208.11784* (2022).
- [45] Q. Guo, S.-B. Zheng, J. Wang, C. Song, P. Zhang, K. Li, W. Liu, H. Deng, K. Huang, D. Zheng *et al.*, *Phys. Rev. Lett.* **121**, 130501 (2018).
- [46] J. Qiu, Y. Zhou, C.-K. Hu, J. Yuan, L. Zhang, J. Chu, W. Huang, W. Liu, K. Luo, Z. Ni *et al.*, *Phys. Rev. Appl.* **16**, 054047 (2021).
- [47] K. M. Fonseca-Romero, S. Kohler, and P. Hänggi, *Chem. Phys.* **296**, 307 (2004).
- [48] K. M. Fonseca-Romero, S. Kohler, and P. Hänggi, *Phys. Rev. Lett.* **95**, 140502 (2005).
- [49] A. Dmitriev and A. Vershovskii, *J. Phys.: Conf. Ser.* **1135**, 012051 (2018).
- [50] A. K. Dmitriev, H. Y. Chen, G. D. Fuchs, and A. K. Vershovskii, *Phys. Rev. A* **100**, 011801(R) (2019).
- [51] A. K. Dmitriev and A. K. Vershovskii, *Phys. Rev. A* **105**, 043509 (2022).
- [52] T. Mikawa, R. Okaniwa, Y. Matsuzaki, and H. Ishi-Hayase, *Phys. Rev. A* **108**, 012610 (2023).
- [53] The controlling axes are chosen as x, y explicitly in our paper; however, we can select any other two perpendicular axes. Additionally, we set $\omega_x = \omega_y$; however, decoupling effects can be obtained by a similar procedure when $\omega_y = n\omega_x$, with $n \in \mathbb{Z}$.
- [54] In this condition, the unitary evolution after one period including two nearest-neighboring intervals becomes
- $$\begin{aligned} \hat{U}_{\text{eff}}^{\text{II}} = & \exp(-i\gamma_2 T \hat{J}_z) \hat{T} \exp\left[-i \int_{T/2}^T \hat{H}_r^{\text{II},2}(t) dt\right] \\ & \times \exp\left(\frac{i\gamma_2 T \hat{J}_z}{2}\right) \exp\left(-\frac{i\gamma_1 T \hat{J}_z}{2}\right) \\ & \times \hat{T} \exp\left[-i \int_0^{T/2} \hat{H}_r^{\text{II},1}(t) dt\right], \end{aligned}$$
- with $\gamma_1 = -\gamma_2$, $|\gamma_j|T/2 = 2n\pi$, and $\hat{H}_r^{\text{II},j} = b_x[\cos(\gamma_j t)\hat{J}_x - \sin(\gamma_j t)\hat{J}_y]$. Then $\hat{U}_{\text{eff}}^{\text{II}} \approx \exp[-i2b_x^2\hat{J}_z/\gamma_2 + O(b_x^2/\gamma_2^2)] \exp[-i2b_x^2\hat{J}_z/\gamma_1 + O(b_x^2/\gamma_1^2)] = \exp[O(b_x^2/\gamma_2^2)]$.
- [55] T.-L. Ho, *Phys. Rev. Lett.* **81**, 742 (1998).
- [56] T. Ohmi and K. Machida, *J. Phys. Soc. Jpn.* **67**, 1822 (1998).
- [57] C. K. Law, H. Pu, and N. P. Bigelow, *Phys. Rev. Lett.* **81**, 5257 (1998).
- [58] D. M. Stamper-Kurn and M. Ueda, *Rev. Mod. Phys.* **85**, 1191 (2013).
- [59] Y. Eto, H. Ikeda, H. Suzuki, S. Hasegawa, Y. Tomiyama, S. Sekine, M. Sadgrove, and T. Hirano, *Phys. Rev. A* **88**, 031602(R) (2013).
- [60] J. R. Petta, A. C. Johnson, J. M. Taylor, E. A. Laird, A. Yacoby, M. D. Lukin, C. M. Marcus, M. P. Hanson, and A. C. Gossard, *Science* **309**, 2180 (2005).
- [61] F. H. Koppens, C. Buizert, K.-J. Tielrooij, I. T. Vink, K. C. Nowack, T. Meunier, L. Kouwenhoven, and L. Vandersypen, *Nature (London)* **442**, 766 (2006).
- [62] J. M. Taylor, J. R. Petta, A. C. Johnson, A. Yacoby, C. M. Marcus, and M. D. Lukin, *Phys. Rev. B* **76**, 035315 (2007).
- [63] V. V. Dobrovitski, J. M. Taylor, and M. D. Lukin, *Phys. Rev. B* **73**, 245318 (2006).
- [64] V. V. Dobrovitski and H. A. De Raedt, *Phys. Rev. E* **67**, 056702 (2003).
- [65] Q. Liu and Y. Zou (private communication).